Mechanical tightening of a synthetic molecular knot

Matteo Calvaresi[1], Anne-Sophie Duwez[2,6*], David A. Leigh[3,4*], Damien Sluysmans[2], Yiwei Song[3,4], Francesco Zerbetto[1*], Liang Zhang[4,5*]

[1] Dipartimento di Chimica "G. Ciamician", Alma Mater Studiorum – Università di Bologna, 40126 Bologna, Italy.

[2] UR Molecular Systems, University of Liège, Sart-Tilman 4000, Belgium.

[3] Department of Chemistry, University of Manchester, Manchester M13 9PL, United Kingdom.

[4] School of Chemistry and Molecular Engineering, East China Normal University, 200062 Shanghai, China.

[5] Shanghai Frontiers Science Center of Molecular Intelligent Synthesis, School of Chemistry and Molecular Engineering, East China Normal University, Shanghai 200062, P.R. China.

[6] Lead contact

*Correspondence: asduwez@uliege.be; david.leigh@manchester.ac.uk; francesco.zerbetto@unibo.it; zhangliang@chem.ecnu.edu.cn

GRAPHICAL ABSTRACT

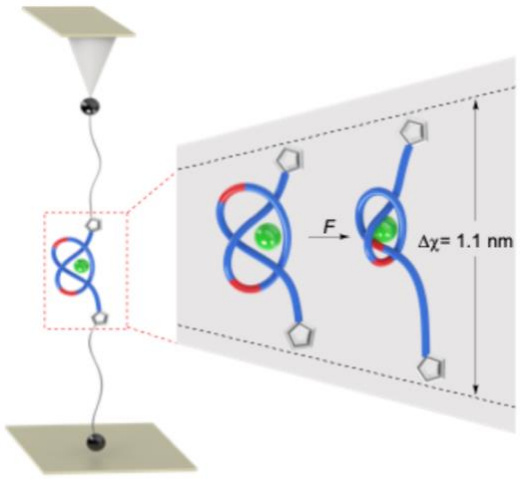

HIGHLIGHTS

- Effects of tightening a synthetic molecular overhand knot by pulling the strands ends apart are revealed by single-molecule force spectroscopy.
- Quantum chemical calculations indicate that the mechanism of tightening involves sliding of part of the entangled region within the knot cavity.
- A lanthanide ion that templates the entanglement remains coordinated during both tightening and the reverse, loosening, process that regenerates the original knotted conformation.

- The presence of the overhand knot increases the extensibility that the strand can accommodate by ~13 kcal mol^{-1} of mechanical stress compared to an unknotted strand.

SUMMARY

Little is known regarding the effects of knotting on the mechanical properties of individual molecules. Here we report on the force response of discrete synthetic small-molecule trefoil knots upon tightening. By combining single-molecule force spectroscopy with QC calculations, we provide evidence for the mechanism of tightening. It is associated with a high resisting force compared to that for larger protein knots and is modulated by the chemical environment. The central metal coordination was found to play a crucial role in the tightening process, and in the reverse process that recovers the initial knotted conformation. Due to the compact structure, the recovery of conformation after mechanical perturbation is very fast. The tightening is also found to play an important role in accommodating mechanical stress. It provides a reserve of extensibility; the extra energy that the knotted strand can absorb in comparison with an unknotted strand is ~13 kcal mol^{-1}.

THE BIGGER PICTURE

Molecular level knots and entanglements occur in DNA, RNA, proteins and polymers of sufficient length and flexibility. However, to date there are few experimental reports on the consequences of molecular knot tightening. Quantifying the response of knots to external stress is central to both their usefulness and limitations. Here, the mechanical response of small-molecule synthetic trefoil knots has been investigated by single-molecule pulling experiments and quantum chemistry calculations. The data provide, for the first time, experimental details concerning the response of well-defined entanglements to an external load. In addition to the rapid reversibility of the tightening process, the tightening force was shown to be modulated in different environments. The results are illustrative of the relative rigidity of such synthetic small-molecule knots, as well as their high resistance to external loads compared to biological knots. The higher extensibility of the knotted molecule, and the extra energy that it can accommodate in response to mechanical perturbations in comparison with an unknotted strand, has relevance for the design of extended knotted and molecularly woven materials.

KEYWORDS

Molecular knot, mechanical properties, single-molecule force spectroscopy, quantum chemistry calculations

INTRODUCTION

At the macroscopic scale, the effect on properties of the mechanical tightening of knots is central to both their usefulness[1,2] (e.g. nooses, stopper knots, etc) and limitations[3,4] (e.g. weakening of strands at the point of knotting to different extents depending on the knot

topology). Molecular level knots and entanglements occur in DNA,[5] RNA,[6] proteins[7] and form spontaneously and randomly in polymers of sufficient length and flexibility.[8] However, to date there are few experimental reports on the consequences of molecular knot tightening.[9-20] Synthetic small-molecule knots are generally compact, with their conformations constrained by the entanglement topology and the number and types of atoms and bonds within the closed-loop strand.[21-41] Entangling molecular strands so that the crossing regions cannot pass through each other blocks pathways to particular conformations and alters strand dynamics. These effects have led to small-molecule knots showing promising properties for anion binding,[42,43] membrane transport,[44] catalysis,[45,46] materials,[47-50] nanotherapeutics[51] and the kinetic stabilization[52] of supramolecular structures.

For more than two decades, single-molecule force spectroscopy (SMFS) has proved efficacious in deciphering mechanistic information of individual biomolecules and in quantifying their force response to external stress[53-55]. SMFS experiments on biological open knots have suggested rationales for some of their biological roles[10-14]. An example of untying a protein slipknot has also been demonstrated[12,17], as well as the tightening of a protein slipknot into a trefoil knot[13]. In addition to its widespread use with biological macromolecules, atomic force microscopy (AFM)-based SMFS has been adapted for the study of synthetic macromolecules including polymers[56], mechanophores[57-60], and interlocked systems[61,62]. However, only a few investigations have been realized on small molecules, successful examples including molecular recognition pairing[63], helical structures[64] and artificial molecular machines prototypes[65-70]. The rarity of such studies stems from the difficulty in developing proper tools and preparing appropriate molecules that can be interfaced with SMFS techniques, especially when one wants to probe sub-molecular motions.

Here we employ AFM-based SMFS and quantum chemical (QC) calculations to probe the mechanics of a synthetic small-molecule trefoil knot, **1** (Figure 1).[30] We study a single strand containing three tridentate 2,6-pyridinebiscarboxamide units that folds around a nine-coordinate Lu^{3+} cation to form an open trefoil (overhand) knot (**1**).[46] We bridge the lanthanide-coordinated overhand knot between a gold substrate and a gold-coated tip of the AFM (Figure 1A). The coordinated Lu^{3+} cation is known[30] to maintain the knotted conformation in solution (Figure 1C). The mechanical response of the knot was investigated in different environments and compared with the unknotted strand. The force required to mechanically tighten the knot was quantitatively measured and the extra energy that the knotted molecule can accommodate in comparison with an unknotted one was estimated. The metal coordination was found to play a crucial role in the tightening process, and in the reverse process that recovers the initial knotted conformation.

RESULTS AND DISCUSSION

Knot synthesis and substrate grafting

The synthesis of overhand knot **1** (chemical structure shown in Figure 1C) followed previously published protocols[46] using lanthanide metal ions as templates to direct the folding of the tri(2,6-pyridinebiscarboxamide) strand in the entanglement of an overhand trefoil knot. To the ends of the strand we added poly(ethylene glycol) (PEG) tethers bearing thiolane end-groups by CuAAC[71] 'click' reactions (Section S1). The addition of the disulfide groups and PEG chains allowed interfacing of the molecules for AFM experiments. The synthetic procedures and characterization data are provided in the SI. Molecules of **1** were grafted in solution onto gold-coated silicon substrates following a strict protocol to attain a low grafting density and favour single-molecule attachments with the tip[68,70].

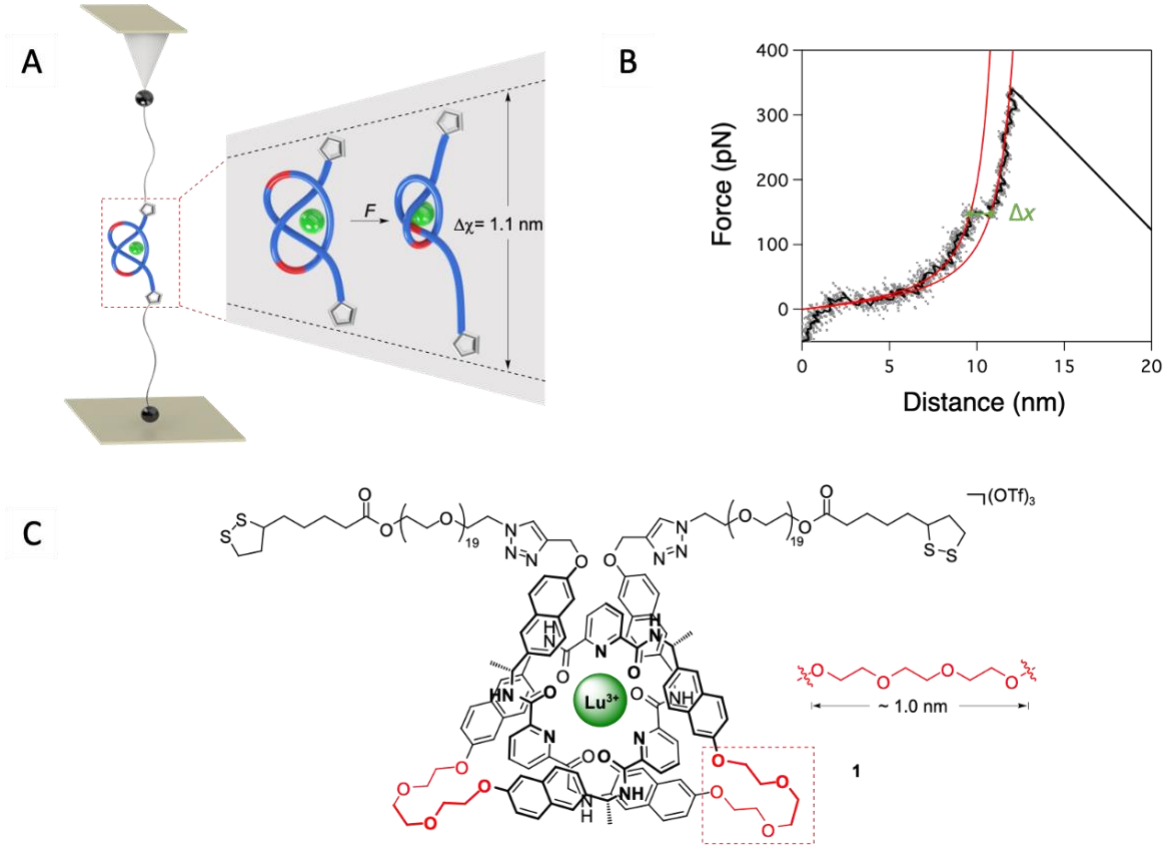

Figure 1. AFM-based single-molecule force spectroscopy on a synthetic overhand knot.

(A), Depiction of the interfacing of the molecular knot between the AFM tip and the substrate. The knot (in blue) conformation is maintained in solution by coordination to Lu^{3+} (in green). Two functional poly(ethylene glycol) chains are used as tethers for the trapping of the knot between the tip and the substrate. The mechanical tightening of the knot is associated with an incremental distance of 1.1 nm.

(B), Characteristic force-distance profile of the knot pulling experiments in 1,1,2,2-tetrachloroethane (TCE) showing a 1-nm pseudo-plateau. Two worm-like chain (WLC) fits are

added in red as a guide to the eye (original to tightened conformation), raw data appear in grey dots and the filtered curve in black.
(C), Chemical structure of overhand knot **1** used for the AFM experiments.

Characteristic force profile

During standard force spectroscopy experiments, the grafted substrate was immersed in 1,1,2,2-tetrachloroethane (TCE) and the AFM tip advanced to approach the surface. A contact force was applied to favour the attachment of the molecule (**1**) onto the tip, then the distance between the tip and the surface was increased in a controlled manner. During the retraction, the force exerted by the interfaced molecule was monitored directly as a deflection of the flexible tip-bearing cantilever (Figure 1A). A typical force-distance curve is displayed in Fig. 1B and features a pattern characteristic of the knot response to the external stress. Control experiments performed on the unknotted molecule display only single-peak profiles (Figure S3) corresponding to the usual worm-like chain[72] (WLC) behaviour of a flexible polymer under load. Conversely, when the knot was stretched, we observed a deviation from the typical WLC behaviour (WLC fits in red in Figure 1B). This characteristic deviation appears either as a small pseudo-plateau or a small peak in the force curve (see also supplementary force curves in Figure S4). As shown in Figure 2A, the incremental distance related to the deviation (Δx) is reproducible, with a most-probable value at 1.1 ± 0.1 nm. The force associated is 103 ± 5 pN (Figure 2B), corresponding to the rupture of weak interactions within the molecular structure. The presence of this characteristic deviation results in an increase in the extensibility of the molecule. The area between the two WLC curves corresponds to the extra energy that the knotted molecule can accommodate[73] in comparison with an unknotted one (Figure 2C), *i.e.* the additional energy that a single chain can sustain under an external force if a molecular knot is incorporated along the chain. We can indeed consider that a polymer chain with a tightened knot is comparable to a single chain of similar length without any knot (in other words, the tightened part does not lead to a length increase upon stretching). This energy was determined to be 13 ± 1 kcal·mol^{-1} in TCE (Figure 2D).

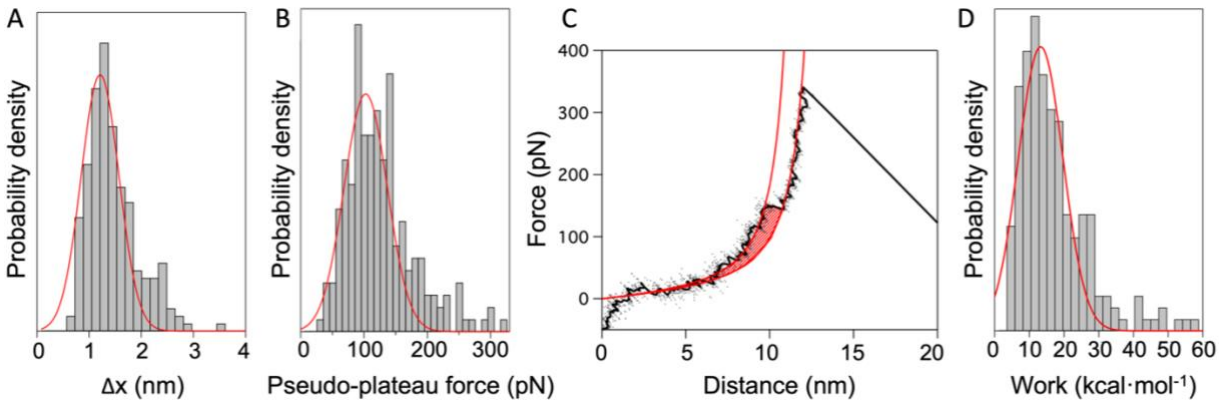

Figure 2. Characteristic deviation length and force distributions in TCE.
(A), Distribution of the length increase (Δx) associated with the characteristic deviation from the WLC behaviour (pseudo-plateaus and small peaks) in TCE. The most probable population is obtained from a multi-gaussian analysis (details in SI) and is centered at 1.1 ± 0.1 nm (in red, N=210).
(B), Distribution of the force of the deviation in TCE. The multi-gaussian analysis returned one main population centered at 103 ± 5 pN (in red, N=210).
(C), Force-distance curve of the knot pulling in TCE fitted with the WLC model (in red) before and after the deviation region. The hatched red area between the two WLC fits represents the extra energy that the single knot molecule can accommodate.[73]
(D), Distribution of the measured value for the hatched area (N=200).

QC calculations and tightening mechanism

In order to relate the characteristic feature observed in the force curves with the detailed behaviour of the molecular knot under load, we performed QC calculations on the Lu^{3+} overhand knot. The calculations excluded the tethers required for the AFM experiments. The geometry of **1** was optimized at each step of the extension (by increasing the distance between the oxygens at both ends of the thread) and the energy of each optimized geometry determined (Figure 3). The values of the energy obtained by the QC calculations describe the potential energy curve along which the AFM experiments take place. As such, they do not consider the entropic components and the dissipation energy related to the process. In the presence of an external force, F, the energy barrier is modified proportional to $F.d$, where d is the displacement.[74] Nevertheless, the calculated evolution of the molecular geometry upon increasing the end-to-end distance is a good illustration of the behaviour of the knot under external load. The energy profile in Figure 3 (top) is associated with the optimized geometries at selected points of the extension (bottom). First, the molecule was aligned along the pulling axis (steps *a* to *c*). The sliding of the first sterically hindered unit, here a naphthalene group, inside the knot cavity occurs between steps *d* and *f*. After this step, the size of the cavity decreases and conformational strain appears on the next naphthalene unit of the chain, impeding the sliding motion of the connecting ethylene glycol units in the cavity (*h* to *j*). A similar variation in energy is observed for both the *d-f* and *g-j* steps. Finally, the energy increases to much higher values for the passing of the second naphthalene unit inside the cavity (*j* to *l*).

Between 40-50 Å of extension (*d* to *i*), the calculations show a sawtooth pattern, consisting of subsequent increases and drops in energy. Figure 3 and Movie S1 show that these steps correspond to the sliding of one arm of the knot (ethylene glycol chain bridging both naphthalene units, in red in Figure 1C) inside the knot cavity. The distance over which this sliding occurs, about 1.2 nm (which corresponds to the length of one arm of the knot), matches the Δx value observed experimentally (1.1 nm).

The combination of the analysis of the QC calculations and the characteristic AFM force profile of Figure 1B map well onto each other and describe the behaviour of the single small-molecule overhand knot under load. First, the force increases following the WLC model, which corresponds to the stretching of the flexible tethers. Once the knot is under tension and the external load is sufficiently high, one arm of the knot slides inside the knot cavity, this step appearing as the characteristic deviation pattern (in green in Figure 1B). The inherent experimental noise prevents the identification of individual steps (sliding of the naphthalene and the ethylene glycol units) or coordination changes during this molecular motion, as evidenced in the QC energy profile. The tightening is complete when the second naphthalene unit reaches the cavity and blocks the sliding, as illustrated in Movie S1 and Figure 3 (step *j*). Then the typical extension of the tethers resumes (second WLC in Fig. 1B) until the detachment of the chain from the AFM tip at higher force.

In recent SMFS studies employing AFM or optical traps to investigate the tightening of open knot proteins, as well as the unknotting of slipknot proteins,[12,13,17] representative force curves associated with the tightening of such proteins generated only one large peak, corresponding to the sliding from the original conformation to the tighten one. The force required to stress protein knots is relatively small (< 20 pN). Here, for the small-molecule synthetic knot (**1**), the original conformation is much more constricted, the molecular dynamics more constrained, and metal-ligand coordination interactions are modified during the tightening process (Section S5). We found that a higher force was required to stress the synthetic small-molecule knot (about 100 pN) compared to protein knots, reflecting the compact entanglement of the small-molecule knot. Each step of the tightening process is taking place at a similar force and over a very small distance, resulting in a force profile that appears as a pseudo-plateau. The appearance of small peaks instead of pseudo-plateaus can be explained by several experimental parameters: the pulling geometry or the fact that the transition occurs in a very short time, approaching the time response of the cantilever and possibly hiding some specific features. Given the very small revealed length considered here (Δx = 1.1 nm), it is not possible or too hazardous to further analyze and distinguish specific behaviours based on the type of profiles.

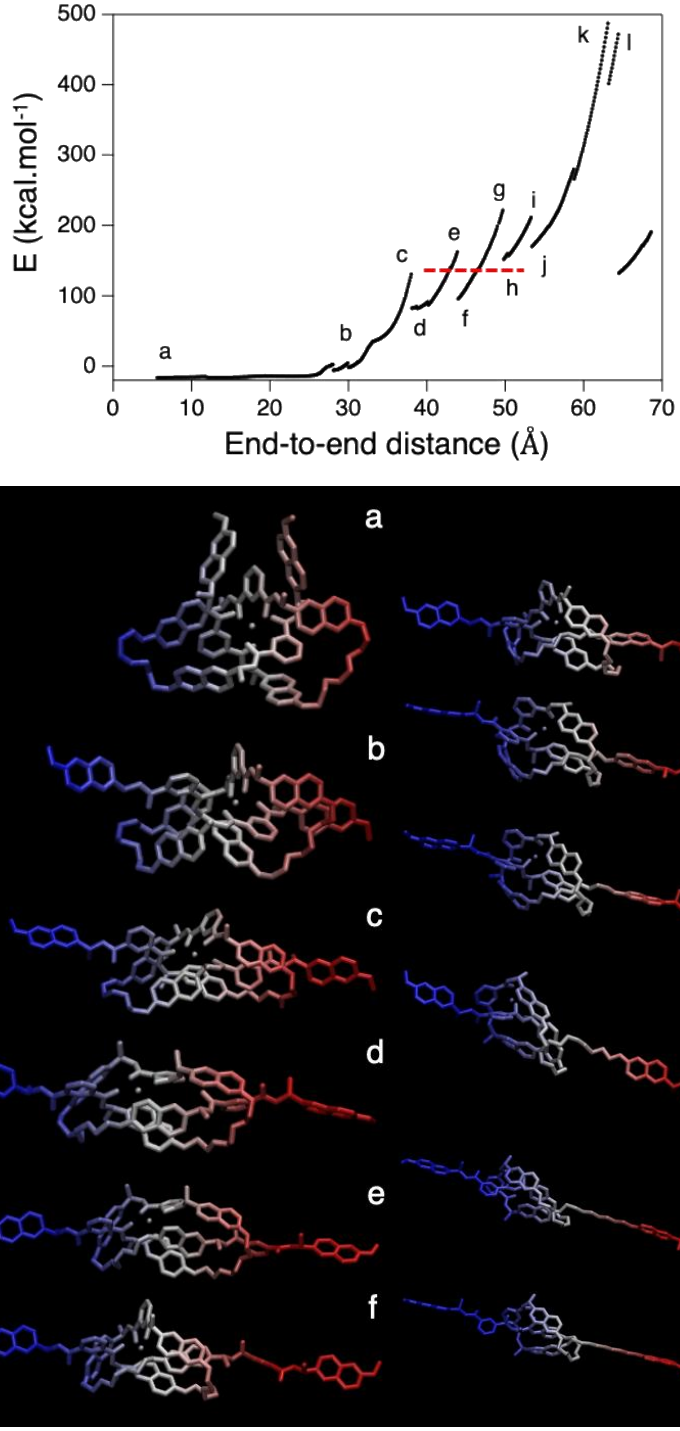

Figure 3. QC calculations of the knot mechanical tightening.

The distance between oxygens at both ends of the knot strand was increased incrementally with the geometry shown at key steps (*a* to *l*). The quantum chemical simulations (details in SI) returned optimized geometries (bottom) and associated energies (top). A saw-tooth profile is observed between steps *d* to *j*, corresponding to the sliding motion of three ethylene glycol units inside the knot cavity. The distance increase from *d* to *j* (in red) matches with the pseudo-plateau extension evidenced during SMFS experiments. In the process, the coordination of the Lu atom changes substantially (Section S5).

Environmental modulation of the knot tightening

The force required to tighten the overhand knot (**1**) was probed in different environments. First, we performed SMFS experiments in a polar solvent, acetonitrile (MeCN). A representative force-distance curve in MeCN is shown in Figure 4A. The force curves display the characteristic deviation with $\Delta x = 1.1 \pm 0.1$ nm (Figure S5A), similar to the characteristic profiles obtained in TCE. The associated force distribution (Figure S5B) presents a population at lower forces (64 ± 4 pN) in MeCN, in complete agreement with the destabilizing effect of this solvent on metal-ligand coordination interactions.[75] A second population of force is also found at 134 ± 16 pN, corresponding to cases when a second 1-nm deviation appears at a higher force (Figure 4B). These profiles correspond to events where the external force is high enough to allow the sliding of the second naphthalene unit within the knot cavity (Figure 3, step *I*), appearing as a second deviation in the force curve. Such behaviours were only observed in MeCN, where the metal-ligand interactions are weakened and the sliding is facilitated despite the overall compactness of the knot structure. The extra energy accommodated by the knotted molecule in MeCN was also determined. The most-probable value observed in MeCN (7 ± 1 kcal·mol^{-1}) (Figure S6) is about half that observed in TCE (13 kcal·mol^{-1}).

Similar pulling experiments performed on **1** in an even more polar solvent, *N,N*-dimethylformamide (DMF), resulted only in single-peak profiles (Figure 4C), without any deviation from the typical WLC behaviour, exactly as observed for the unknotted molecule (Figure S3). The absence of the characteristic knot tightening profile indicates that the coordination interactions have been disrupted in solution, likely causing unknotting of the molecule prior to the AFM attachment. This untangling is supported by similar ^{1}H NMR spectra for the knotted strand and a linear (*i.e.* unknotted) strand in DMF-d$_7$ (Figure S2). We can thus conclude that the solvent has a strong effect on the stability of the overhand knot, from the destabilizing of the intramolecular interactions that maintain the entangled structure in MeCN to the complete unknotting of the molecule in DMF.

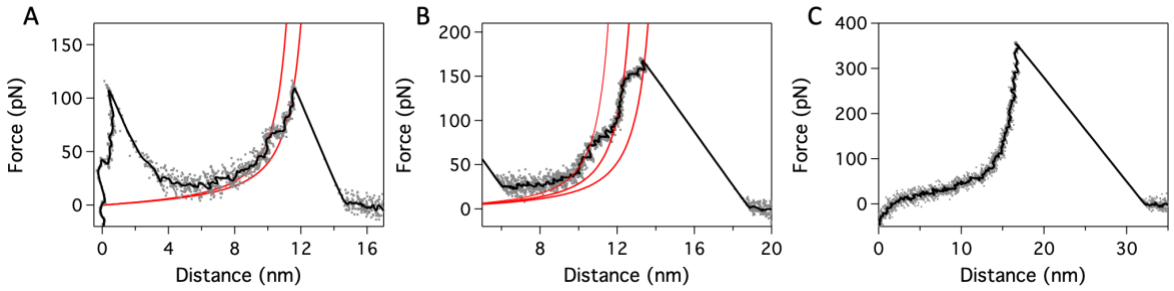

Figure 4. Modulation of the knot tightness in three environments.

(A), Characteristic force-distance curve of the knot stretched in acetonitrile (MeCN). The deviation length (Figure S5A) is similar to that observed in TCE, but the force is lower (64 ± 4 pN, Figure S5B), evidencing the destabilization of the original knot conformation in this polar

solvent.
(B), Representative force curve with a double deviation profile obtained in MeCN. The second 1-nm deviation explains the origin of the second force population observed in Figure S5B and corresponds to the sliding of the second naphthalene unit inside the mechanically constrained knot cavity.
(C), Characteristic force-distance curve observed for the knot in *N,N*-dimethylformamide (DMF) illustrated by the loss of the characteristic deviation of the knotted conformation in favour of a typical single-peak profile associated with an unknotted conformation.
WLC fits, in red, are added as a guide to the eye. Raw data appear in grey dots and filtered curves in black.

Reversibility of the mechanical tightening

We investigated the reversibility of the mechanical tightening process by performing pulling-relaxing experiments in TCE. Such custom force measurements consist of stretching a single molecule up to a threshold force higher than the tightening force, but without detaching the molecule from the tip. Once this force is reached, the external load is reduced by approaching the tip back to the surface in a controlled manner (Section S4). In other words, the knot is successively tightened and then loosened. During the pulling process (Figure 5, blue trace), we observed the characteristic tightening of the knot discussed previously. The relaxing process (red trace) revealed a similar pattern, *i.e.* a characteristic deviation similar to the one observed in the pulling curve. This behaviour is different from previous experiments performed on knot proteins, where the relaxing curve did not display evidence for reversible dynamics,[14] or at much lower forces.[15,17,18] A closer look at the QC calculations at large end-to-end distances revealed a distortion of the aromatic moieties in the optimized geometries (Figure 3). The presence of this conformational strain in addition to the compactness of the knot may be what facilitates the observation of this reverse sliding of the chain, back to the original conformation. It is also clear evidence that the Lu^{3+} ion remains within the knot and is not expelled from the cavity during the tightening process, but modifies its coordination (Section S5) during the tightening and stretching process.

These experiments highlight the high stability and fast recovery of the knot conformation after mechanical perturbation. We note that the reverse motion shows very little or no hysteresis compared to the mechanical tightening, indicative of a non-dissipative pathway.

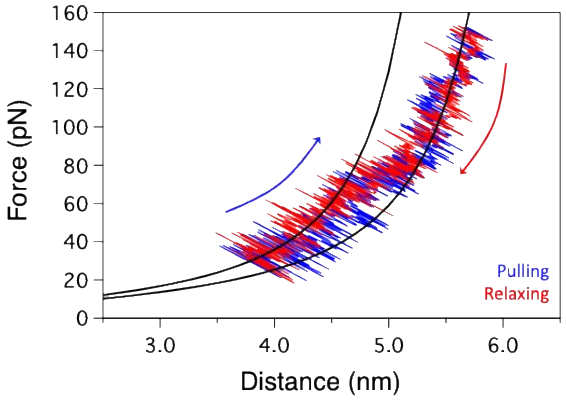

Figure 5. Single-molecule pulling-relaxing experiments in TCE show the reversibility of the knot tightening.

The pulling movement starts away from the substrate (4 nm away from the contact point) with a single knot trapped between the tip and the surface. The pulling trace (in blue, raw data) shows the characteristic deviation profile corresponding to the mechanical tightening of the knot. The extension is stopped before the molecule detaches from the tip, and the tip is then moved back towards the surface (relaxing curve in red, raw data). An identical profile is observed during the relaxing part, including the reverse deviation. At the end of the relaxing part, the force profile follows the original WLC curve (black trace) corresponding to the behaviour of the knot before mechanical tightening.

DISCUSSION

The mechanical response of a small-molecule synthetic trefoil overhand knot (**1**) has been investigated by single molecule AFM pulling experiments. QC calculations provide optimized geometries at various increasing extensions of the strand that provide a tightening mechanism consistent with the experimental results. The force spectroscopy data show a characteristic deviation from the typical stretching of a polymer chain, a pattern corresponding to the sliding of one arm of the knot within its cavity, in agreement with the pathway indicated by the QC calculations. Advanced force measurements demonstrate that the metal ion remains bound within the knot during the tightening experiments, aiding the facile recovery of the original knotted strand conformation with no or very little hysteresis. In addition to the rapid reversibility of the tightening process, the knot's tightening force is modulated in different environments. The results are illustrative of the relative rigidity of such synthetic small-molecule knots, as well as their high resistance to external loads compared to biological knots. They also provide, for the first time, experimental details concerning the response of such topologies to an external load. The higher extensibility of the knotted molecule and the extra energy that it can accommodate in response to mechanical perturbations in comparison with an unknotted strand should be relevant for the designs of extended knotted and woven 2D[48] and 3D[49,50] materials.

EXPERIMENTAL PROCEDURES

Resource Availability

Lead Contact

Anne-Sophie Duwez, asduwez@uliege.be

Materials Availability

This study did not generate new reagents.

Data and Code Availability

The force profiles from AFM measurement are available on request from A.-S.D.; QM calculation data is available on request from F.Z.

SUPPLEMENTAL INFORMATION

The supplemental information can be found at:

ACKNOWLEDGMENTS

D.S. is a Postdoctoral Researcher of the F.R.S.-FNRS (Chargé de recherches). The research was supported by the PDR T.0075.21 project of the FRS-FNRS at University of Liège. L.Z. and D.A.L. thank East China Normal University for funding. L.Z. thanks the National Natural Science Foundation of China (22001074) and the Shanghai Sailing Program (20YF1411400) for funding. D.A.L. is a Royal Society Research Professor.

AUTHOR CONTRIBUTIONS

D.S., L.Z., A.-S.D. and D.A.L. designed the experiments. Y.S and L.Z. carried out the chemical synthesis and characterization studies. D.S. performed the AFM experiments and analyzed the data. M.C. and F.Z. performed the QC calculations. A.-S.D. and D.A.L. directed the research. D.S. wrote the initial draft of the manuscript. All the authors discussed the results and commented on the manuscript.

DECLARATION OF INTERESTS

The authors declare no competing interests.

REFERENCES

1. Ashley, C. (1994). The Ashley Book of Knots (Doubleday).

2. Maddocks, J.H. and Keller, J.B. (1987). Ropes in equilibrium. SIAM J. Appl. Math. *47*, 1185–1200.

3. Pieranski, P., Kasas, S., Dietler, G., Dubochet, J. and Stasiak, A. (2001). The rupture of knotted strings under tension. New J. Phys. *3*, 10.
4. Patil, V.P., Sandt, J.D., Kolle, M. and Dunkel, J. (2020). Topological mechanics of knots and tangles. Science *367*, 71–75.
5. Meluzzi, D., Smith, D.E. and Arya, G. (2010). Biophysics of knotting. Annu. Rev. Biophys. *39*, 349–366.
6. Zhao, M. and Woodside, M.T. (2021). Mechanical strength of RNA knot in Zika virus protects against cellular defenses. Nat. Chem. Biol. 17, 975–981.
7. Lim, N.C.H. and Jackson, S.E. (2015). Molecular knots in biology and chemistry. J. Phys. Condens. Matter *27*, 354101.
8. Frank-Kamenetskii, M.D., Lukashin, A.V. and Vologodskii, A.V. (1975). Statistical mechanics and topology of polymer chains. Nature *258*, 398–402.
9. Saitta, A.M., Soper, P.D., Wasserman, E. and Klein, M.L. (1999). Influence of a knot on the strength of a polymer strand. Nature *399*, 46–48.
10. Arai, Y., Yasuda, R., Akashi, K., Harada, Y., Miyata, H., Kinosita, K.J. and Itoh, H. (1999). Tying a molecular knot with optical tweezers. Nature *399*, 446–448.
11. Bornschlogl, T., Anstrom, D.M., Mey, E., Dzubiella, J., Rief, M. and Forest, K.T. (2009). Tightening the knot in phytochrome by single-molecule atomic force microscopy. Biophys. J. *96*, 1508–1514.
12. He, C., Genchev, G.Z., Lu, H. and Li, H. (2012). Mechanically untying a protein slipknot: multiple pathways revealed by force spectroscopy and steered molecular dynamics simulations. J. Am. Chem. Soc. *134*, 10428–10435.
13. He, C., Lamour, G., Xiao, A., Gsponer, J. and Li, H. (2014). Mechanically tightening a protein slipknot into a trefoil knot. J. Am. Chem. Soc. *136*, 11946–11955.
14. Ziegler, F., Lim, N.C.H., Mandal, S.S., Pelz, B., Ng, W.-P., Schlierf, M., Jackson, S.E. and Rief, M. (2016). Knotting and unknotting of a protein in single molecule experiments. Proc. Natl. Acad. Sci. USA *113*, 7533–7538.
15. Bustamante, A., Sotelo-Campos, J., Guerra, D.G., Floor, M., Wilson, C.A.M., Bustamante, C. and Baez, M. (2017). The energy cost of polypeptide knot formation and its folding consequences. Nat. Commun. *8*, 1581.
16. Xu, Y., Li, S., Yan, Z., Luo, Z., Ren, H., Ge, G., Huang, F. and Yue, T. (2018). Stabilizing effect of inherent knots on proteins revealed by molecular dynamics simulations. Biophys. J. *115*, 1681–1689.
17. He, C., Li, S., Gao, X., Xiao, A., Hu, C., Hu, X., Hu, X. and Li, H. (2019). Direct observation of the fast and robust folding of a slipknotted protein by optical tweezers. Nanoscale *11*, 3945–3951.
18. Wang, H. and Li, H. (2020). Mechanically tightening, untying and retying a protein trefoil knot by single-molecule force spectroscopy. Chem. Sci. *11*, 12512–12521.

19. Bao, Y., Luo, Z. and Cui, S. (2020). Environment-dependent single-chain mechanics of synthetic polymers and biomacromolecules by atomic force microscopy-based single-molecule force spectroscopy and the implications for advanced polymer materials. Chem. Soc. Rev. *49*, 2799–2827.
20. Zhang, L., Lemmonier, J.-F., Acocella, A., Calvaresi, M., Zerbetto, F. and Leigh, D.A. (2019). Effects of knot tightness at the molecular level. Proc. Natl. Acad. Sci. USA *116*, 2452–2457.
21. Forgan, R.S., Sauvage, J.-P. and Stoddart, J.F. (2011). Chemical topology: complex molecular knots, links, and entanglements. Chem. Rev. *111*, 5434–5464.
22. Ayme, J.-F., Beves, J.E., Campbell, C.J. and Leigh, D.A. (2013). Template synthesis of molecular knots. Chem. Soc. Rev. *42*, 1700–1712.
23. Fielden, S.D.P., Leigh, D.A. and Woltering, S.L. (2017). Molecular knots. Angew. Chem. Int. Ed. *56*, 11166–11194.
24. Dietrich-Buchecker, C.O. and Sauvage, J.-P. (1989). A synthetic molecular trefoil knot. Angew. Chem. Int. Ed. Engl. *28*, 189–192.
25. Brüggemann, J., Bitter, S., Müller, S., Müller, W.M., Müller, U., Maier, N.M., Lindner, W. and Vögtle, F. (2007). Spontaneous knotting—From oligoamide threads to trefoil knots. Angew. Chem. Int. Ed. *46*, 254–259.
26. Guo, J., Mayers, P.C., Breault, G.A. and Hunter, C.A. (2010). Synthesis of a molecular trefoil knot by folding and closing on an octahedral coordination template. Nat. Chem. 2, 218–222.
27. Barran, P.E., Cole, H.L., Goldup, S.M., Leigh, D.A., McGonigal, P.R., Symes, M.D., Wu, J. and Zengerle, M. (2011). Active-metal template synthesis of a molecular trefoil knot. Angew. Chem. Int. Ed. *50*, 12280–12284.
28. Ponnuswamy, N., Cougnon, F.B.L., Clough, J.M., Pantoş, G.D. and Sanders, J.K.M. (2012). Discovery of an organic trefoil knot. Science *338*, 783–785.
29. Ayme, J.-F., Beves, J.E., Leigh, D.A., McBurney, R.T., Rissanen, K. and Schultz, D. (2012). A synthetic molecular pentafoil knot. Nat. Chem. 4, 15–20.
30. Zhang, G., Gil-Ramirez, G., Markevicius, A., Browne, C., Vitorica-Yrezabal, I.J. and Leigh, D.A. (2015). Lanthanide template synthesis of trefoil knots of single handedness. J. Am. Chem. Soc. *137*, 10437–10442.
31. Danon, J.J., Krüger, A., Leigh, D.A., Lemonnier, J.-F., Stephens, A.J., Vitorica-Yrezabal, I.J. and Woltering, S. L. (2017). Braiding a molecular knot with eight crossings. Science 355, 159–162.
32. Zhang, L., August, D.P., Zhong, J., Whitehead, G.F.S. Vitorica-Yrezabal, I.J. and Leigh, D.A. (2018). Molecular trefoil knot from a trimeric circular helicate. J. Am. Chem. Soc. 140, 4982–4985.

33. Cougnon, F.B.L., Caprice, K., Pupier, M., Bauza, A. and Frontera, A. (2018). A strategy to synthesize molecular knots and links using the hydrophobic effect. J. Am. Chem. Soc. *140*, 12442–12450.
34. Segawa, Y., Kuwayama, M., Hijikata, Y., Fushimi, M., Nishihara, T., Pirillo, J., Shirasaki, J., Kubota, N. and Itami, K. (2019). Topological molecular nanocarbons: All-benzene catenane and trefoil knot. Science *365*, 272–276.
35. Zhang, H.-N., Gao, W.-X., Lin, Y.-J. and Jin, G.-X. (2019). Reversibly structural transformation between a molecular Solomon link and an unusual unsymmetrical trefoil knot. J. Am. Chem. Soc. *141*, 16057–16063.
36. Dang, L.-L., Feng, H.-J., Lin, Y.-J. and Jin, G.-X. (2020). Self-assembly of molecular figure-eight knots induced by quadruple stacking interactions. J. Am. Chem. Soc. *142*, 18946–18954.
37. Leigh, D.A., Schaufelberger, F., Pirvu, L., Stenlid, J.H., August, D.P. and Segard, J. (2020). Tying different knots in a molecular strand. Nature *584*, 562–568.
38. Inomata, Y., Sawada, T. and Fujita, M. (2020). Metal-peptide torus knots from flexible short peptides. Chem *6*, 294–303.
39. Leigh, D.A., Danon, J.J., Fielden, S.D.P., Lemonnier, J.-F., Whitehead, G.F.S. and Woltering, S. L. (2021). A molecular endless (7_4) knot. Nat. Chem. *13*, 117–122.
40. Song, Y., Schaufelberger, F., Ashbridge, Z., Pirvu, L., Vitorica-Yrezabal, I.J. and Leigh, D.A. (2021). Effects of turn-structure on folding and entanglement in artificial molecular overhand knots. Chem Sci. *12*, 1826–1833.
41. Ashbridge, Z., Kreidt, E., Pirvu, L., Schaufelberger, F., Halldin Stenlid, J., Abild-Pedersen, F. and Leigh, D.A. (2022). Vernier template synthesis of molecular knots. Science *375*, 1035–1041.
42. Ayme, J.-F., Beves, J.E., Campbell, C.J., Gil-Ramírez, G., Leigh, D.A. and Stephens, A.J. (2015). Strong and selective anion binding within the central cavity of molecular knots and links. J. Am. Chem. Soc. *137*, 9812−9815.
43. Bilbeisi, R.A., Prakasam, T., Lusi, M., El-Khoury, R., Platas-Iglesias, C., Charbonnière, L.J., Olsen, J.-C., Elhabiri, M. and Trabolsi, A. (2016). [C–H···anion] interactions mediate the templation and anion binding properties of topologically non-trivial metal-organic structures in aqueous solutions. Chem. Sci. *7*, 2524−2532.
44. August, D.P., Borsley, S., Cockroft, S.L., della Sala, F., Leigh, D.A. and Webb, S.J. (2020). Transmembrane ion channels formed by a Star of David [2]catenane and a molecular pentafoil knot. J. Am. Chem. Soc. *142*, 18859−18865.
45. Marcos, V., Stephens, A.J., Jaramillo-Garcia, J., Nussbaumer, A.L., Woltering, S.L., Valero, A., Lemonnier, J.-F., Vitorica-Yrezabal, I.J. and Leigh, D. A. (2016). Allosteric initiation and regulation of catalysis with a molecular knot. Science *352*, 1555–1559.
46. Gil-Ramírez, G., Hoekman, S., Kitching, M.O., Leigh, D.A., Vitorica-Yrezabal, I.J. and Zhang, G. (2016). Tying a molecular overhand knot of single handedness and asymmetric

catalysis with the corresponding pseudo-D_3-symmetric trefoil knot. J. Am. Chem. Soc. *138*, 13159–13162.
47. Katsonis, N., Lancia, F., Leigh, D.A., Pirvu, L., Ryabchun, A. and Schaufelberger, F. (2020). Knotting a molecular strand can invert macroscopic effects of chirality. Nat. Chem. *12*, 939–944.
48. August, D.P., Dryfe, R.A.W., Haigh, S.J., Kent, P.R.C., Leigh, D.A., Lemonnier, J.-F., Li, Z., Muryn, C.A., Palmer, L.I., Song, Y., Whitehead, G.F.S. and Young, R.J. (2020) Self-assembly of a layered two-dimensional molecularly woven fabric. Nature 588, 429–435.
49. Liu, Y., Ma, Y., Zhao, Y., Sun, X., Gándara, F., Furukawa, H., Liu, Z., Zhu, H., Zhu, C., Suenaga, K. et al. (2016). Weaving of organic threads into a crystalline covalent organic framework. Science *351*, 365–369.
50. Zhang, Z.-H., Andreassen, B.J., August, D.P., Leigh, D.A and Zhang, L. (2022). Molecular weaving. Nat. Mater. *21*, 275–283.
51. Benyettou, F., Prakasam, T., Nair, A.R., Witzel, I.-I., Alhashimi, M., Skorjanc, T., Olsen, J.-C., Sadler, K.C. and Trabolsi, A. (2019). Potent and selective *in vitro* and *in vivo* antiproliferative effects of metal-organic trefoil knots. Chem. Sci. *10*, 5884–5892.
52. Leigh, D.A., Pirvu, L., Schaufelberger, F., Tetlow, D.J. and Zhang, L. (2018). Securing a supramolecular architecture by tying a stopper knot. Angew. Chem. Int. Ed. *57*, 10484–10488.
53. Duwez, A.-S. and Willet, N. (2012). Molecular Manipulation with Atomic Force Microscopy (CRC Press, Boca Raton).
54. Clausen-Schaumann, H., Seitz, M., Krautbauer, R. and Gaub, H.E. (2000). Force Spectroscopy with Single Bio-Molecules. Curr. Opin. Chem. Biol. *4*, 524−530.
55. Müller, D.J., Dumitru, A.C., Giudice, C.L., Gaub, H.E., Hinterdorfer, P., Hummer, G., De Yoreo, J.J., Dufrêne, Y.F. and Alsteens, D. (2021). Atomic Force Microscopy-based force spectroscopy and multiparametric imaging of biomolecular and cellular systems. Chem. Rev. *121*, 11701–11725.
56. Bao, Y., Luo, Z. and Cui, S. (2020). Environment-dependent single-chain mechanics of synthetic polymers and biomacromolecules by atomic force microscopy-based single-molecule force spectroscopy and the implications for advanced polymer materials. Chem. Soc. Rev. *49*, 2799−2827.
57. Brown, C. and Craig, S.L. (2015). Molecular engineering of mechanophore activity for stress-responsive polymeric materials. Chem. Sci. *6*, 2158−2165.
58. Ghanem, M.A., Basu, A., Behrou, R., Boechler, N., Boydston, A.J., Craig, S.L., Lin, Y., Lynde, B.E., Nelson, A., Shen, H. and Storti, D.W. (2021). The role of polymer mechanochemistry in responsive materials and additive manufacturing. Nat. Rev. Mater. *6*, 84−98.
59. Bowser, B.H., Wang, S., Kouznetsova, T.B., Beech, H.K., Olsen, B.D., Rubinstein, M. and Craig, S.L. (2021). Single-event spectroscopy and unravelling kinetics of covalent domains based on cyclobutane mechanophores. J. Am. Chem. Soc. *143*, 5269−5276.

60. Zhang, Y., Wang, Z., Kouznetsova, T.B., Sha, Y., Xu, E., Shannahan, L., Fermen-Coker, M., Lin, Y., Tang, C. and Craig, S.L. (2021). Distal conformational locks on ferrocene mechanophores guide reaction pathways for increased mechanochemical reactivity. Nat. Chem. *13*, 56−62.
61. Janke, M., Rudzevich, Y., Molokanova, O., Metzroth, T., Mey, I., Diezemann, G., Marszalek, P.E., Gauss, J., Böhmer, V. and Janshoff, A. (2009). Mechanically interlocked Calix[4]arene dimers display reversible bond breakage under force. Nat. Nanotechnol. *4*, 225−229.
62. Xing, H., Li, Z., Wang, W., Liu, P., Liu, J., Song, Y., Wu, Z.L., Zhang, W. and Huang, F. (2019). Mechanochemistry of an interlocked poly[2]catenane: from single molecule to bulk gel. CCS Chem. *1*, 513−523.
63. Sluysmans, D., Zhang, L., Li, X., Garci, A., Stoddart, J.F. and Duwez, A.-S. (2020). Viologen tweezers to probe the force of individual donor-acceptor π-interactions. J. Am. Chem. Soc. *142*, 21153−21159.
64. Devaux, F., Li, X., Sluysmans, D., Maurizot, V., Bakalis, E., Zerbetto, F., Huc, I. and Duwez, A.-S. (2021). Single-molecule mechanics of synthetic aromatic amide helices: ultrafast and robust non-dissipative winding. Chem *7*, 1333−1346.
65. Lussis, P., Svaldo-Lanero, T., Bertocco, A., Fustin, C.-A., Leigh, D.A. and Duwez, A.-S. (2011). A single synthetic small molecule that generates force against a load. Nat. Nanotechnol. *6*, 553−557.
66. van Quaethem, A., Lussis, P., Leigh, D.A., Duwez, A.-S. and Fustin, C.-A. (2014). Probing the mobility of catenane rings in single molecules. Chem. Sci. *5*, 1449−1452.
67. Naranjo, T., Lemishko, K.M., de Lorenzo, S., Somoza, A., Ritort, F., Peŕez, E. and Ibarra, B. (2018). Dynamics of individual molecular shuttles under mechanical force. Nat. Commun. *9*, 4512.
68. Sluysmans, D., Hubert, S., Bruns, C.J., Zhu, Z., Stoddart, J.F. and Duwez, A.-S. (2018). Synthetic oligorotaxanes exert high forces when folding under mechanical load. Nat. Nanotechnol. *13*, 209−213.
69. Sluysmans, D., Devaux, F., Bruns, C.J., Stoddart, J.F. and Duwez, A.-S. (2018). Dynamic force spectroscopy of synthetic oligorotaxane foldamers. Proc. Natl. Acad. Sci. USA *115*, 9362−9366.
70. Sluysmans, D., Lussis, P., Fustin, C.-A., Bertocco, A., Leigh, D.A. and Duwez, A.-S. (2021). Real-time fluctuations in single-molecule rotaxane experiments reveal an intermediate weak binding state during shuttling. J. Am. Chem. Soc. *143*, 2348−2352.
71. Rostovstev, V.V., Green, L.G., Fokin, V.V. and Sharpless, K.B. (2002). A stepwise Huisgen cycloaddition process: Copper(I)-catalyzed regioselective ligation of azides and terminal alkynes. Angew. Chem. Int. Ed. *41*, 2596−2599.
72. Marantan, A. and Mahadevan, L. (2018). Mechanics and statistics of the worm-like chain. Am. J. Phys. *86*, 86−94.

73. Marszalek, P.E., Oberhauser, A.F., Pang, Y.-P. and Fernandez, J.M. (1998). Polysaccharide elasticity governed by chair-boat transitions of the glucopyranose ring. Nature *396*, 661–664.
74. Howard, J. (2001). Mechanics of motor proteins and the cytoskeleton (Sinauer Assoc.).
75. Hunter, C.A. (2004). Quantifying intermolecular interactions: guidelines for the molecular recognition toolbox. Angew. Chem. Int. Ed. *43*, 5310–5324.